

Electronic structure of Si(111)-7×7 phase boundary studied by scanning tunneling microscopy

Koji Miyake and Hidemi Shigekawa^{a)}

Institute of Materials Science, University of Tsukuba, Tsukuba 305, Japan

Ryuzo Yoshizaki

Cryogenics Center, University of Tsukuba, Tsukuba 305, Japan

(Received 3 January 1995; accepted for publication 2 April 1995)

Remarkably low electron density of Si adatoms at the Si(111)-7×7 phase boundary was found by scanning tunneling microscopy. The observed charge transfer was apparent with sample bias voltages down to ~ -0.8 eV, close to the value of the dangling bond state of the rest atoms in the Si(111) 7×7 surface. In consideration of the DAS (dimer-adatom-stacking fault) model, the observed charge transfer could be related to the structural change in the dimer layer caused by phase mismatching at the boundary. In fact, such charge transfer was not observed at the less disordered boundaries formed by introducing 5×5 half unit cells. Similar large charge transfer was found to occur in the quenched disordered 1×1 structure. These results agree with the similar chemical reactivity observed in the two disordered structures. © 1995 American Institute of Physics.

In the chemical reaction processes occurring on material surfaces, electronic structure of the substrate surfaces is known to play essential roles. As Avouris *et al.* showed in atom-resolved surface chemistry by scanning tunneling microscopy (STM), initial reactive sites and subsequent reactions of oxygen and NH₃ molecules on Si surfaces were governed by the local electronic structure of the substrates.^{1,2} For charge transfer between adsorbates and substrates, the importance of the energy level structure of the substrate surface was shown by the analysis of the high-resolution photoemission spectroscopy spectrum for the alkali metal adsorption onto Si surfaces.³ These properties are also very important in understanding, for example, the processes of atomic layer epitaxy⁴ and initial growth of compound semiconductors.⁵ Therefore, in order to design and control the material structure on an atomic scale, it is very important to characterize and understand the influential local electronic structures of material surfaces/interfaces.

Recently, in the molecular beam epitaxial growth of Si and Ge on Si(111) 7×7 substrate, the nucleation and growth modes of Si or Ge islands were found to be strongly affected by the existence of the phase boundary.⁶⁻⁸ Despite the important roles of the local electronic structure as mentioned above, STM studies performed on the Si(111)-7×7 domain boundaries have clarified only the arrangement of the first-layer adatoms.⁹⁻¹² In addition, the formation and relaxation mechanisms of the stacking fault are essential with regarding to the Si(111)-7×7 surface reconstruction.⁸ Therefore, analysis of the phase boundary, including underlayers, is very important from both practical and fundamental points of view.

In this letter, with consideration of the bias-voltage-dependent STM images, the structure of the Si(111)-7×7 phase boundary will be discussed in detail on the basis of the DAS (dimer-adatom-stacking-fault) model.¹³

Phosphorous-doped (1 Ω cm) Si(111) sample surfaces were prepared by conventional heat treatment following a one-day prebake. Base pressure was $\sim 1.0 \times 10^{-8}$ Pa, and

pressure during the heat treatment was kept below $\sim 5 \times 10^{-8}$ Pa. STM was performed at room temperature using an electrochemically etched tungsten tip, and all STM images shown in this letter were obtained in the constant current mode.

Figures 1(a) and 1(b) show empty-state (sample bias: $V_s = 2.0$ V), tunneling current: $I_t = 300$ pA) and filled-state ($V_s = -2.0$ V, $I_t = 300$ pA) STM images of a Si(111)7×7 phase boundary, respectively. The phase boundary is indicated by A–A in the figures. Phase mismatching at the boundary is apparent in the empty-state image, as shown in Fig. 1(a); however, adatoms at the boundary are as bright as those in the regular 7×7 regions. On the other hand, STM images of adatoms at the boundary are darker and vague in the filled-state image, as shown in Fig. 1(b), indicating lower electron density of the adatoms at the boundary region. Since adatoms with higher electron density were not observed

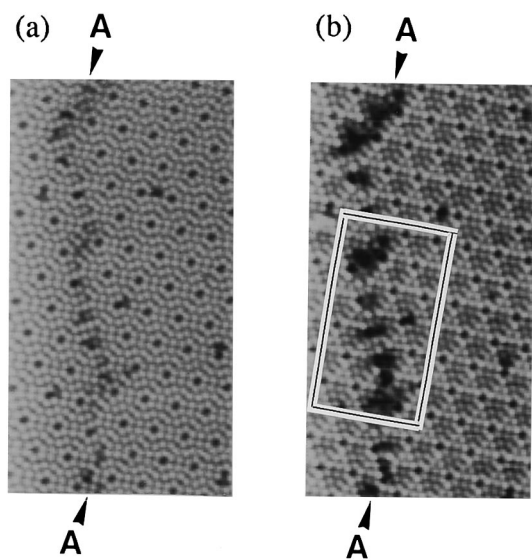


FIG. 1. STM images of domain boundary for (a) empty state ($V_s = 2.0$ V, $I_t = 300$ pA) and (b) filled state ($V_s = -2.0$ V, $I_t = 300$ pA).

^{a)}Electronic mail: hidemi@mat.ims.tsukuba.ac.jp

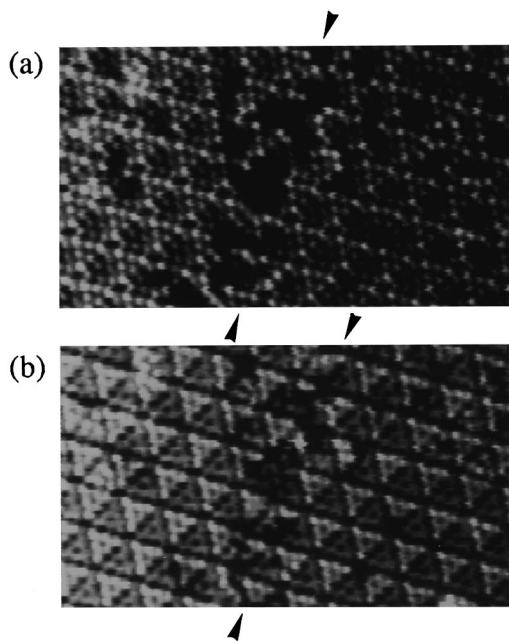


FIG. 2. STM images of a domain boundary obtained at [(a) $V_s = -0.5$ V and (b) $V_s = -1.0$ V]. Tunneling current was 300 pA.

around the boundary, the observed charge transfer is considered to be occurring from the adatoms to the underlayers.

Among the adatoms in a regular 7×7 unit cell, center adatoms are known to be less brighter than the corner adatoms, because center adatoms are surrounded by twofold rest atoms; thereby, the amount of the charge transfer to the rest atoms is larger for the center adatoms than the corner adatoms.^{1,2} Therefore, a possible explanation for the observed bias-dependent STM images is that formation of dimers in the DAS structure was interrupted by the phase mismatching at the boundary, and additional dangling bonds were created along the boundary. When the number of dangling bonds surrounding adatoms is increased at the domain boundary compared to the regular 7×7 surface, larger charge transfer from adatoms to the dangling bond states is expected to make the adatoms in the boundary region darker in the filled-state images.

In order to examine our model, we measured the bias-dependent image of the phase boundary. Figures 2(a) and 2(b) show two filled-state STM images of a boundary obtained at different negative sample bias voltages V_s [(a) -0.5 V and (b) -1.0 V]. As shown in Fig. 2(a), adatoms at the boundary are dark at $V_s = -0.5$ V; however, they become less dark, as shown in Fig. 2(b) when the bias voltage was increased to over -0.8 eV, the energy level of the rest atom dangling bond state.¹⁴

Figures 3(a) and 3(b) show a magnified image and structural model of the squared area in Fig. 1(b). Faulted and unfaulted sites are indicated by F and U in Fig. 3(b), respectively. Since the 7×7 structure is known to be formed from the unfaulted half and the isolated faulted-half structure is unstable, the structure of the boundary region was assumed to be unfaulted here. Dark adatoms at the phase boundary in the filled-state image and the extra rest atoms formed around

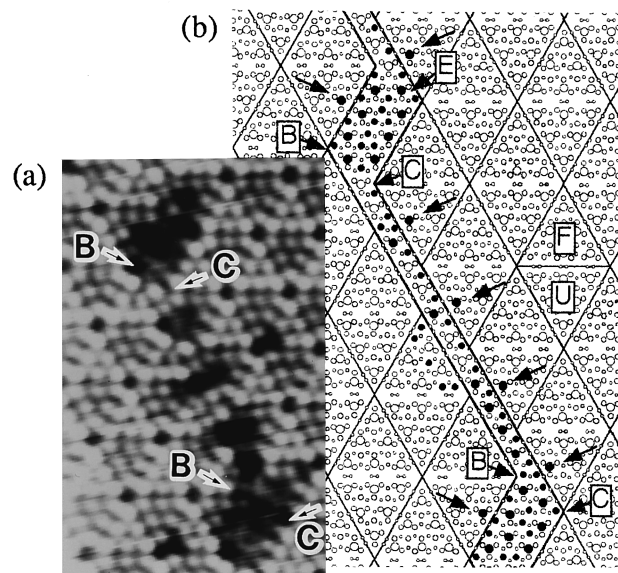


FIG. 3. Magnified image (a) and its structural model (b) of the squared area in Fig. 1.

the boundary are indicated by large and small solid circles in Fig. 3(b), respectively.

According to the DAS model, dimers are formed between the faulted and the unfaulted halves of a 7×7 DAS unit. For the left-hand side of the boundary, since the faulted-half unit cells of the left 7×7 domain are in contact with the boundary which has unfaulted structure, dimers remain along B–B, as shown in Fig. 3(b). On the other hand, in the right domain, unfaulted halves of the 7×7 units are neighboring the unfaulted structure of the boundary. Therefore, atoms on the edge of the unfaulted-half unit cells along C–C in Fig. 2 cannot form dimers and remain as rest atoms, as indicated by solid circles along C–C. As we expected, adatoms between the two lines B–B and C–C are dark, indicating the existence of charge transfer. However, adatoms situated near the corner adatoms of the 7×7 units in the right domain are brighter, which corresponds to the fact that the number of rest atoms surrounding the corner adatoms are relatively small. All the center adatoms in the right domain along the boundary indicated by arrows in Fig. 3 are influenced by the boundary and are darker than other center adatoms as shown in Fig. 3, as expected. In a larger phase boundary area indicated by E, there are many dangling bonds, as shown in Fig. 3. Therefore, we can expect more dark adatoms in this area compared to the boundary between B–B and C–C, which in fact was observed, as shown in Fig. 3(a).

In consideration of the DAS model, it is possible to form a phase boundary with less disturbance of the Si-dimer layer. One possible way is to introduce 5×5 half unit cells, as is schematically shown in Fig. 4(a). Since dimers remain in this case, and the number of rest atoms surrounding the 5×5 adatoms is close to that of the corner adatoms in a regular 7×7 structure, charge transfer at the 5×5 half unit cell may be similar to that at the corner adatoms. In fact, such a boundary was observed by STM, as shown in Fig. 4(b), and all adatoms in the 5×5 half unit cells were as bright as the corner adatoms in the 7×7 unit cells even for the filled-state

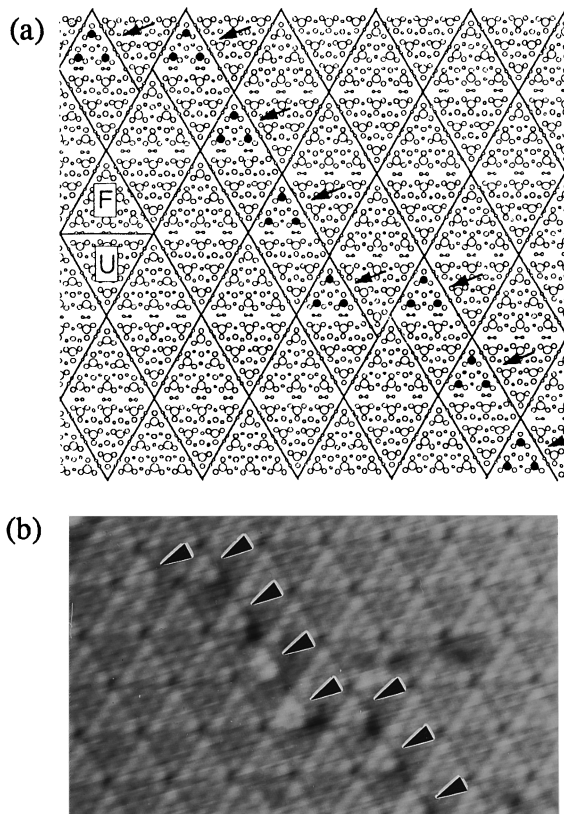


FIG. 4. A structural model (a) and an STM image (b) of a domain boundary formed by introducing 5×5 half unit cells, $V_s = -2.0$ V, $I_t = 300$ pA.

images, as expected. This rule was well verified for the structures formed by mixture of other 7×7 families appearing on the quenched Si(111) surfaces.

Similar large bias-voltage dependence was observed for the disordered triangular 1×1 phase,¹⁵ as is shown in Fig. 5.

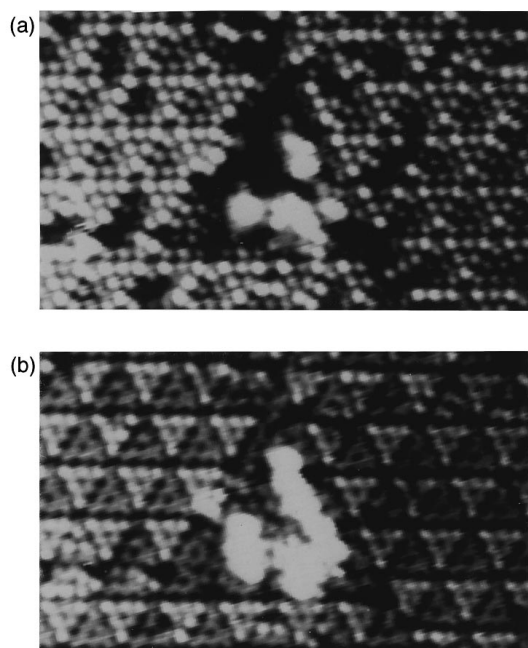


FIG. 5. STM images of a disordered 1×1 triangular structure, (a) $V_s = -0.5$ V, $I_t = 300$ pA and (b) $V_s = -1.0$ V, $I_t = 300$ pA.

The empty-state image of the adatoms in the disordered area was as bright as that of other adatoms in the regular 7×7 area; however, their filled-state image was apparently dark for bias voltages down to ~ -0.8 V. Recently, a quenched Si(111) surface was imaged by atomic force microscopy (AFM) in air, and 7×7 domain boundaries and disordered 1×1 structures associated with the phase transition from 1×1 to 7×7 were similarly observed as protrusions 0.1–0.15 nm higher than the regular 7×7 region, indicating similar surface reactivity of these structures.¹⁶ Extra atoms on the top layer were bright for both bias polarities, indicating a metallic electronic structure. The triangular 1×1 phase structure has not been clarified yet; however, similar charge transfer to that at the phase boundary may explain the similar chemical reactivity observed by the AFM measurement for these two disordered areas. According to our model, dimers seem to be formed at the boundary.

In summary, lower charge density of the top-layer Si atoms at the Si(111)- 7×7 phase boundary was found by studying the bias-voltage-dependent STM images. On the basis of the DAS model at the phase boundary, the change in the electronic structure could be attributed to the charge transfer caused by the disorder in the dimer layer at the phase boundary. Phase boundary with less disorder formed by introducing 5×5 half unit cells was found to exist, the STM image of which was explained well by our model. Similar large charge transfer was found to occur at the disordered 1×1 triangular structure formed by quenching. These results are consistent with the similar chemical reactivity observed for these two disordered structures.

This work was supported in part by a Grant-in-Aid for Scientific Research from the Ministry of Education, Science and Culture of Japan. Research Foundation for Materials Science is also acknowledged.

¹ Ph. Avouris and R. Wolkow, Phys. Rev. B **39**, 5091 (1989).

² Ph. Avouris, I.-W. Lyo, and F. Bozso, J. Vac. Sci. Technol. B **9**, 424 (1991).

³ Y. Ma, C. T. Chen, G. Meigs, F. Settee, G. Illing, and H. Shigekawa, Phys. Rev. B **45**, 5961 (1992).

⁴ K. Uesugi, T. Takiguchi, M. Izawa, M. Yoshimura, and T. Yao, Jpn. J. Appl. Phys. **32**, 6200 (1993).

⁵ H. Shigekawa, H. Oigawa, K. Miyake, Y. Aiso, Y. Nannichi, Y. Hashizume, and T. Sakurai, Appl. Phys. Lett. **65**, 607 (1994).

⁶ U. Köhler, J. E. Demuth, and R. J. Hamers, J. Vac. Sci. Technol. A **7**, 2860 (1989).

⁷ U. Köhler, O. Jusko, G. Pietsch, B. Müller, and M. Henzler, Surf. Sci. **248**, 321 (1991).

⁸ W. Shimada and H. Tochiara, Hyomen Kagaku **15**, 535 (1994); Surf. Sci. **311**, 107 (1994).

⁹ H. Tanaka, M. Udagawa, M. Itoh, T. Uchiyama, Y. Watanabe, T. Yokosuka, and I. Sumita, Ultramicroscopy **42-44**, 864 (1992).

¹⁰ M. J. Hadley and S. P. Tear, Surf. Sci. Lett. **247**, L221 (1991).

¹¹ I. Sumita, T. Yokokawa, H. Tanaka, M. Udagawa, Y. Watanabe, M. Takao, and K. Yokoyama, Appl. Phys. Lett. **57**, 1313 (1990).

¹² J. E. Demuth, R. J. Hamers, R. M. Tromp, and M. E. Welland, J. Vac. Sci. Technol. A **4**, 1320 (1986).

¹³ K. Takayanagi, Y. Tanishiro, M. Takahashi, and S. Takahashi, J. Vac. Sci. Technol. A **3**, 1502 (1985).

¹⁴ R. J. Hamers, R. M. Tromp, and J. E. Demuth, Phys. Rev. Lett. **56**, 1972 (1986).

¹⁵ Y. N. Yang and E. D. Williams, Phys. Rev. Lett. **72**, 1862 (1994).

¹⁶ T. Fukuda, Jpn. J. Appl. Phys. **33**, 6A, 797 (1994).